Article:

Alizadeh, M, Hassanpour, A orcid.org/0000-0002-7756-1506, Pasha, M et al. (2 more authors) (2017) The effect of particle shape on predicted segregation in binary powder mixtures. Powder Technology, 319. pp. 313-322. ISSN 0032-5910

https://doi.org/10.1016/j.powtec.2017.06.059

The effect of particle shape on predicted segregation in binary powder mixtures

Mohammadreza Alizadeh, Ali Hassanpour*, Mehrdad Pasha, Mojtaba Ghadiri, Andrew Bayly.
School of Chemical and Process Engineering, University of Leeds, Leeds, UK.
*Corresponding author:
Tel: +44(0)113 343 2405
A.Hassanpour@leeds.ac.uk

Abstract
NEW

Particle shape driven segregation in particulate mixtures has received limited attention in the literature either experimentally or via simulation. This study investigates the shape driven segregation which occurs during the process of heap formation and evaluates the ability of different Discrete Element Method (DEM) simulation approaches to predict the effect. It shows experimentally that the difference in particle shape can drive segregation in a binary mixture and that this segregation can be predicted by DEM models which resolve the particle shape. In this case shape is resolved via a clumped sphere approach. Importantly, the work also demonstrates that simpler models using spherical particles, with rolling friction calibrated to reproduce the experimental angle of repose, tend to underestimate the segregation tendency. The system studied was a binary mixture of irregular shaped particles, a typical spray dried detergent powder and a granulated detergent additive; particle shapes were obtained using X-ray microtomography.

Key words: Granular segregation, DEM, Discrete Element Method, clumped spheres, rolling friction, spray dried powder, binary mixture

1 Introduction

Segregation is a serious problem in the handling and manufacturing of particulate solid mixtures. It causes a variety of difficulties and has significant cost implications. For example, segregation may impose extra costs, where loss of homogeneity of the formulated mixtures can lead to customer dissatisfaction and/or batch failure due to quality assurance examination [1, 2]. There are many contributing factors leading to segregation; these can be divided into two main categories: 1) differences in particle properties (internal causes) and 2) process dynamics (external causes). From the internal causes, differences in size, density, shape, and surface properties are some of the main factors contributing to segregation [3-6]. For the external causes, vibration [7], shear strain [8], fluid drag [9], and equipment geometry [10], are examples causing segregation by percolation, sifting, projection, and elutriation mechanisms [3, 4, 11-17].

The effect of various parameters on segregation in bounded heap formation is reviewed by Fan et al. [18]. The authors concluded that there is still lack of a profound understanding of the effect of particle shape on segregation, particularly during the particle discharge and heap formation. Rounded particles have a higher flowability, leading to smaller repose angles and more prone to segregation. In contrast irregular shapes are subject to entanglement and interlocking among the particles, preventing them from free flowing and percolations [3, 4, 18-21]. Shape can also be a complementary cause to other segregation-inducing factors such as density and surface condition. For example, shape has a direct impact on packing density of the particles which potentially is a source for segregation [19]. Particle shape can also change the surface to volume ratio of the particles which ultimately affects the influence of the surface condition on particles movement. On this basis, ignoring the shape in numerical simulations may cause misleading results [22]. Numerical simulations are helpful in understanding of segregation phenomenon and its underlying mechanisms. The effects of size and density on segregation have been studied extensively [4, 12, 23-29]; however studies including the shape effect are limited to those which use a rolling friction term as a surrogate for shape and studies which use realistic particle shapes are not widely reported [1, 30].

A common approach to consider the effect of shape has been the use of an artificial rolling friction in the modelling [4, 31-34], which can be calibrated against experimental data. Alternatively a more rigorous approach is to simulate particles shape by clumping spheres together, as proposed by Favier et al. [35], and optimise conformity with the real shape. Nevertheless the use of spheres with calibrated rolling friction in DEM simulations is more prevalent simply because this method is less computationally expensive. Recently, Pasha et al. [36] have shown that the rolling friction can be tuned to simulate the experimental trends, but the shortcoming of this approach is that the optimum value of rolling friction coefficient is not available a priori, and hence the approach is not predictive. Instead, approximating the particle shape by clumped spheres has shown a good agreement with the experimental data [36]. The main objective of this study is to assess the significance of particle shape in numerical simulations of segregation of binary granular mixtures.

A step-by-step methodology for predicting the granular segregation tendency is proposed which has accommodated the particle shape complexity into the simulations. The process of heap formation of a binary powder mixture of spray dried detergent powders (referred to as Blown Powder or BP) and tetraacetylethylenediamine (TAED) particles is simulated using DEM. The approaches of clumped spheres and spheres with calibrated rolling friction are utilised in the simulations and the particle segregation tendency is analysed. The results are then compared qualitatively and quantitatively with the experimental data.

2 Methodology

2.1 Geometry and materials

The geometry used in the simulations and experiments is shown in Fig. 1. It consists of a transparent box (0.200 m in height, 0.191 m in width, and 0.016 m in depth) made from Perspex and a plastic funnel on top. The particles are discharged from the funnel and make a heap in the box from which the repose angle is measured. The same process and geometry is used in DEM simulations in which the angle of repose is used as a benchmark for calibration of the DEM input parameters. All the simulation tests are carried out with a 50:50 balk volume ratio of BP and TAED.

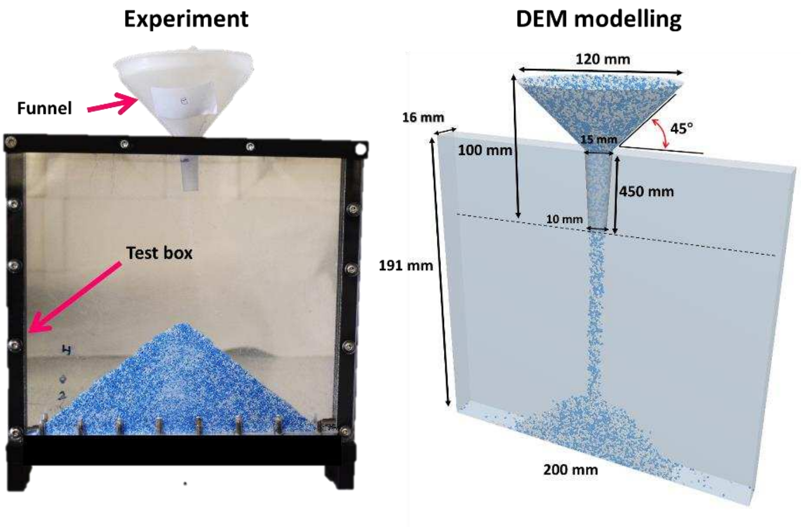

Fig. 1. Geometry utilised in DEM simulations based on the geometry of the experimental set up.

Particles selected and tested here are shown in Fig. 2. BP particles are more irregular, because of the spray drying process, compared to the TAED particles with smaller asperities made by granulation. To ensure that the effect of particle shape on segregation extent is not dominated by the particle size effect, narrow size cuts, 850-1000 µm, of BP and TAED particles were prepared by sieving and used in the experiments.

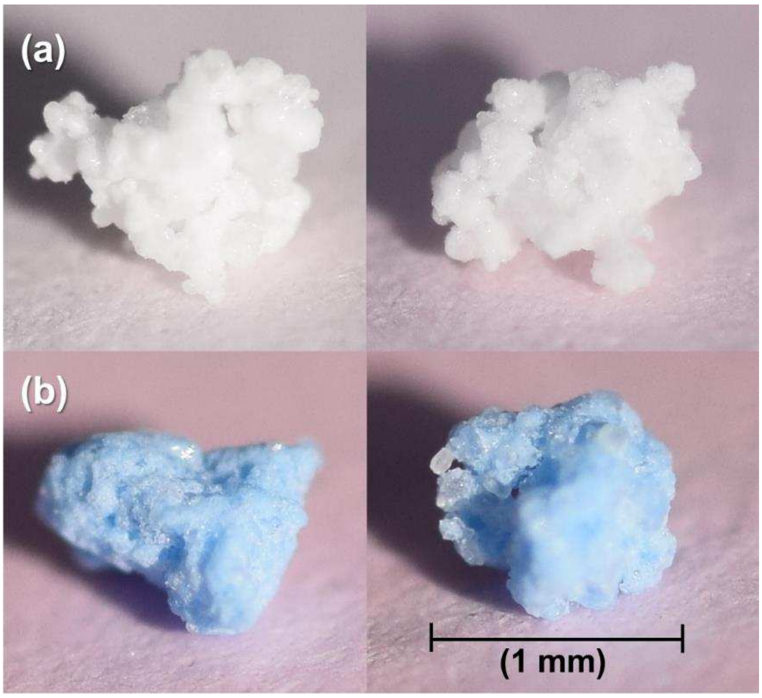

Fig. 2. Typical shapes of (a) BP (white) and (b) TAED (blue) particles sieved between 850 and 1000 µm.

2.2 Computational methodology

EDEM 2.7.0 software provided by DEM Solutions, Edinburgh, UK is used for the simulations. The particles used in this study are dry and free flowing and their sizes are relatively large; therefore the contact adhesive interactions are not dominant and hence negligible compared to the gravitational force (high Bond and low Cohesion numbers) [33, 37]. On this basis, only the Hertz-Mindlin (no slip) [38-40] contact model is applied, where the normal contact force is calculated from the Hertz theory [39] and the tangential component from Mindlin model [40]. The details of these models are available elsewhere [41-43].

Particle shape can be accounted by different approaches, namely clumped spheres and rolling friction. For the clumped spheres approach, the shape is generated by clumping spheres together in a way that the relative positions of the spheres are maintained constant throughout the simulations [35]. A single clumped-sphere particle may contain spheres with different diameters, but the total envelope volume as well as the position of the centre of gravity of the clumped spheres are the same as those of the original particle shape. For the rolling friction approach, particles are all spheres having a resisting torque against their relative free rolling [31]. The rolling friction coefficient defines how much the particles are prevented from free rolling.

2.3 Mechanical and physical properties characterisation

One important part of DEM modelling is to set appropriate physical and mechanical properties for the simulation. In this work efforts have been made to characterise the physical and mechanical parameters as much as possible, as described below.

2.3.1 Restitution coefficient

The coefficient of restitution, CoR, is an important input parameter used in DEM to account for damping of energy of oscillations. In case of collision of objects CoR is the ratio of the rebound relative velocity to the impact velocity. Its value depends upon many factors, such as particle size, material type, internal structure, surface adhesion, speed of collisions, etc. In this study, the CoR of each type of particles against a wall made of Perspex is measured by using a high speed camera and image analysis. A particle is selected randomly and then released from a certain height. The incident and rebound velocities are then determined by image analysis from which the CoR is calculated. This procedure is repeated 12 times and the average of the CoR is selected as the final value. The results are presented in Table 1 together with other properties. Determining CoR of particle-particle collisions is more difficult, as efforts are required to align the particles for collisions and due to particle roughness, a wide spread in the measured values are expected. Considering that for the particles used in this system the values of CoR for particle-wall is small indeed, we used the same value for the inter-particle collisions.

2.3.2 Sliding friction

For non-spherical particles with asperities/surface roughness, the characterisation of the coefficient of sliding inter-particle friction, CoF, is difficult and subject to large variations. We follow an approach in which a simple sliding process of two layers of particles adhered to a plane is simulated by DEM and compared against the experiment. To find the particle-particle CoF, two flat plates are covered by monolayers of particles and are placed on each other as shown in Fig. 3 (a). Then they are tilted together until the upper surface slides and the angle at which the sliding occurs is measured (Fig. 3 (b)). The same process is simulated in DEM using surfaces covered by monolayers of clumped spheres. The surfaces are placed on top of each other and then tilted together. The sliding angle is then compared with the experiment and the CoF is tuned to predict and match the observed sliding angle of the plates.

To measure the CoF of the particles against the wall, a monolayer of the particles is glued to a flat plate and placed over a plain surface made from Perspex. When the surfaces are tilted, at a certain angle (Fig. 3 (c)), the upper surface, with the particles glued on, starts to slide. The tangent of this angle is taken as the coefficient of sliding friction between particles and wall.

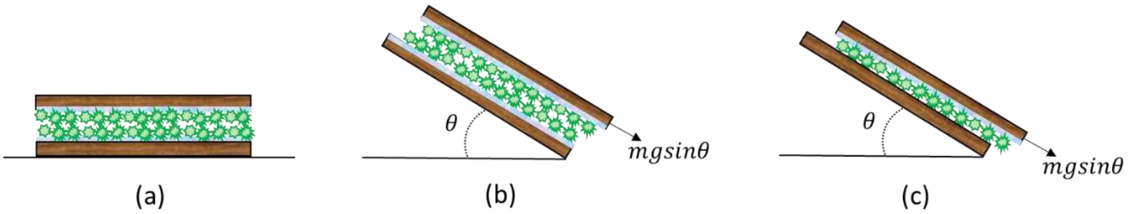

Fig. 3. Schematic diagram for measuring the coefficient of sliding friction. Graph (a) shows the surfaces at rest, graph (b) shows the particle-particle sliding friction experiment, and graph (c) depicts the particle-wall sliding experiment.

Table 1: Physical properties of BP and TAED particles used in DEM simulations.

Material	TAED	BP	wall
Sieve-cut size (μm)	850-1000	850-1000	-
Density (kg/m^3)	1000	1000	1190
Shear modulus (MPa)	10	10	100
Poisson's ratio	0.25	0.25	0.25
CoR (BP-Particle/wall)	0.30	0.20	0.28
CoR (TAED-Particle/wall)	0.32	0.30	0.32
CoF (BP-particle/wall)	0.69	0.62	0.42
CoF (TAED-particle/wall)	0.76	0.69	0.36
CRF	0.01	0.01	0.01

2.4 Characterisation and modelling of particle shape

Due to irregularity of BP and TAED particle shape, the X-ray Tomography (XRT) technique is used to capture the 3D images of particles. Particles from each material are randomly selected and scanned using the Phoenix Nanotom XMT machine at the University of Leeds. The 3D images are then post-processed using the Avizo 3D software, where the 2D X-ray images from different layers of the particle are composed to construct the 3D geometry as shown in Fig. 4. This geometry is then imported into the Automatic Sphere-clump Generator (ASG) software [44], where the clumped spheres are generated based on the obtained particle shape. The generated particle shape can include different numbers of spheres clumped together as shown in Fig. 4. To have a better representation of the real shape a large number of small spheres are needed; however using them in the simulation leads to more computational effort, due to the increase in the number of elements and shorter computational time steps required for smaller particles. Therefore some optimisation of the size and number of clumped spheres is necessary to simulate the phenomenon under consideration reliably and efficiently [36]. In this work the arrangement of clumped spheres, as shown in Fig. 4, has been evaluated considering the same volume and centre of mass as of the real particle.

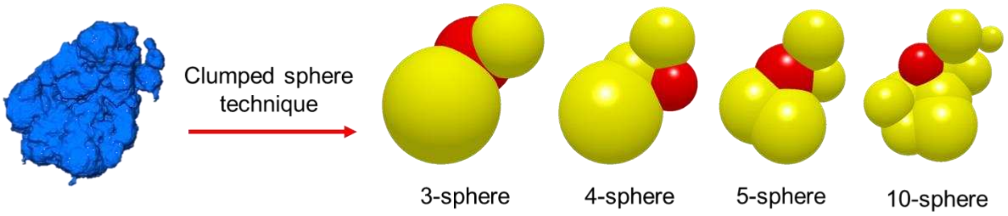

Fig. 4. The non-spherical TAED particle shape representation by increasing the number of spheres (TAED particles' size range: 850-1000 μm).

Clumped sphere approach

To assess the sensitivity of simulation results to the number of spheres used in each clump, the angle of repose of the representative particles is simulated and benchmarked against the experiments. In this study, one particle shape is selected for each species representing the typical shapes of the particles. Also, the effect of rolling friction is minimised by keeping the values of the coefficient of rolling friction constant at 0.01 for all the simulations.

As an example, the repose angle of TAED particles with 5-sphere clumps is depicted in Fig. 5. The optimum sphere number for shape modelling of each type of powder is then determined from the aforementioned sensitivity analysis (Fig. 6). Using 5-clumped sphere particles in the modelling, the angle of repose obtained from the simulation is 36.2°$\pm$0.5°, which is very close to the 36.0°$\pm$1° from the experimental result of TAED particles. Hence the 5-clumped sphere shape is selected for shape representation since it has enough accuracy with lower computational cost compared to the 10-sphere system. The same analysis has been carried out for BP particles, where the minimum number of spheres required to match the experimental angle of repose is also 5 (Fig. 6). Nevertheless, the 8-sphere clump was used for the BP particles in this study due to the presence of a very small sphere in 5-sphere clump, which led to smaller time step for the 5-sphere particle compared to the 8-sphere.

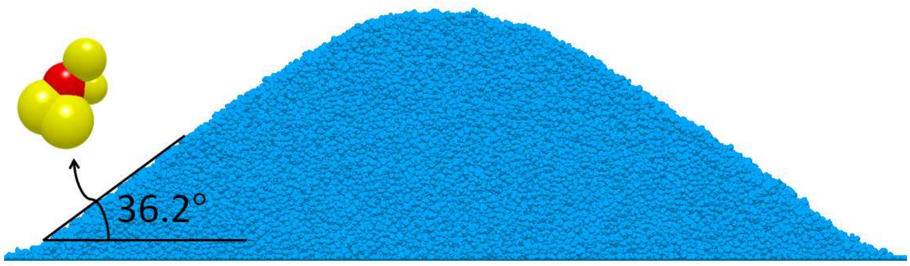

Fig. 5. DEM simulation of a TAED particle heap using 5-sphere clump model. (Particle size range: 850-1000 μm).

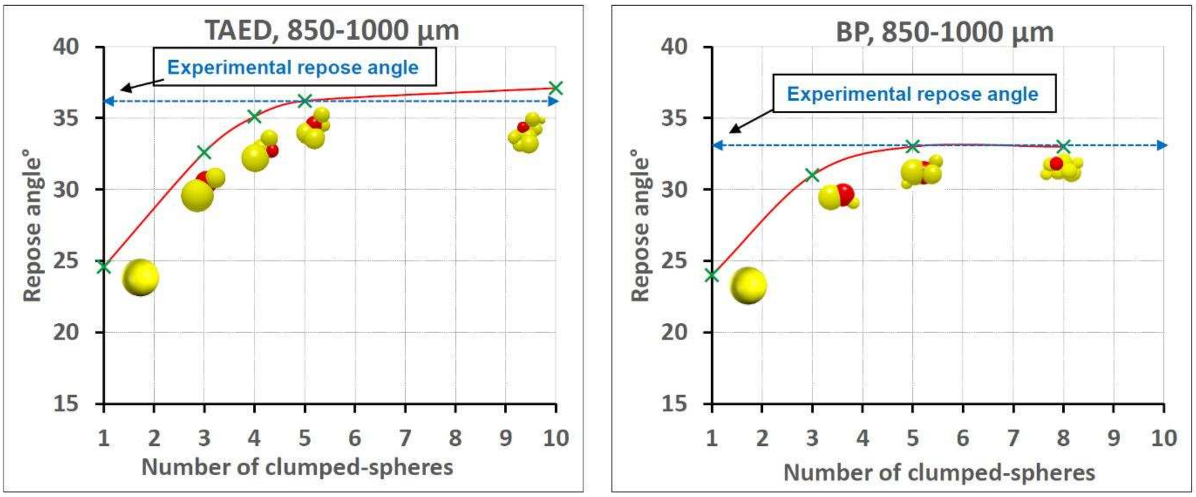

Fig. 6. The effect of number of spheres in the clumped-spheres model on the heap repose angle

The general details and specifications of the modelling and particle shapes used in the simulations are listed in Table 2.

Table 2: Specifications of the modelling and particle shape.

Material		TAED	BP
Number of particles		57902	52098
Total mass (g)		25	32
Particle shape		5-sphere	8-sphere
Equivalent-volume diameter (μm)		938	1058
Repose angle (°)	Simulation	36.2	33.0
	Experiment	36.0	33.0

Rolling friction approach

The use of rolling friction coefficient to account for the effect of particle shape has been reported previously [31, 45]; however, its applicability for modelling the segregation has not been addressed so far. A series of simulations are carried out by investigating the role of rolling friction on the angle of repose, comparing and matching with the experimental data. The volume-equivalent diameter of the particles, d_V, is used for these simulations as given in Table 2. The process of heap formation of particles is simulated for low (0.01), medium (0.05), and high (0.10) values of coefficient of rolling friction as shown in Fig. 7. The calibrated value of rolling friction coefficient is determined using the trend line obtained from the graph. This helps to estimate the value for the coefficient of rolling friction after which another simulation is carried out to ensure that this rolling friction coefficient does give the desired angle of repose. The values for calibrated coefficient of rolling friction are given in Table 3.

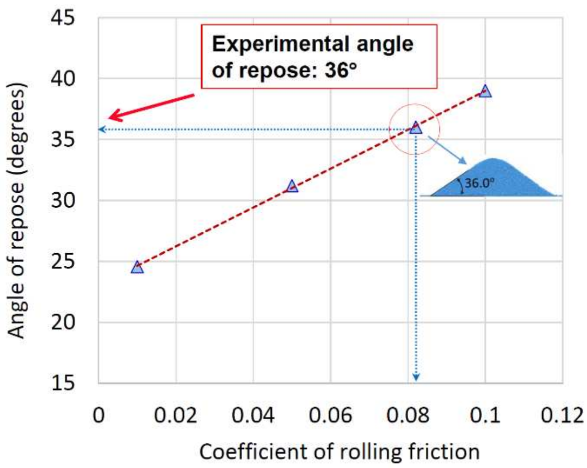

Fig. 7. The procedure of calibrating the spheres rolling friction against the angle of repose.

Table 3: Calibrated coefficient of rolling friction for the spherical particles.

Material	TAED	BP	Wall (Perspex)
BP	0.073	0.064	0.064
TAED	0.082	0.073	0.082

2.5 Segregation analysis

For quantification of the extent of segregation image analysis is used in this work. When the particles are distinguishable by their colours, as is the case here, image analysis is a fast technique as it is easy to apply and less expensive compared to the other techniques [1]. Another advantage of image analysis is that it can be used for both experiment and numerical simulation, allowing a consistent comparison between the results.

Indices to quantify segregation are the same as those used to quantify the degree of mixing within a mixture. There are various segregation indices available most of which are based on variance [46-52]. In the current study, both the segregation pattern (particles concentration distribution) as well as the segregation intensity are significant. The first one is obtained by calculating the concentration of each species in different positions and the latter from the normalised variation of the particles concentration known as the coefficient of variation (CoV). This is also known as the Relative Standard Deviation (RSD) and is one of the mixing indices used extensively to describe the extent of segregation [52-54]. Also the lowest possible CoV for this system in randomly mixed mode is calculated to compare with the segregated system.

2.5.1 Quantifying segregation using image analysis

Heap formation of a binary mixture of BP and TAED particles is simulated using the physical and mechanical properties given in Tables 1-3, and the clumped spheres and rolling friction approaches are compared. The particles are generated in the funnel and then released into the test box to make the heap (Fig. 1). As shown in Fig. 2, BP and TAED particles are in different colours, which allow for detecting their positions in the binary mixture by image analysis. After the heap is formed, the segregation is analysed by the image analysis method.

To find the segregation extent, an image is taken from the front view of the heap which is then divided into several square bins as shown in Fig. 8. The image analysis method developed by Pasha et al. [55] is used here. The number of pixels of each constituent in each bin is calculated by which their pixels number concentrations are determined. The CoV of these pixel concentrations is then calculated for the whole heap. The effect of bin size on CoV of the constituents is also assessed by using different numbers of bins in the analysis. As expected, larger bins give smaller CoV; however based on the case under study and its application, bin size should be neither too large nor too small. In this study, the bins are squares with 10 mm sides, selected to be roughly 10 times wider than the size of one particle. CoV values normally range from zero to one, meaning no segregation (an ideal and totally mixed case) for values close to zero and highly segregated system for one and greater (Equation 1). This approach is applied to both experimental as well as simulated heaps.

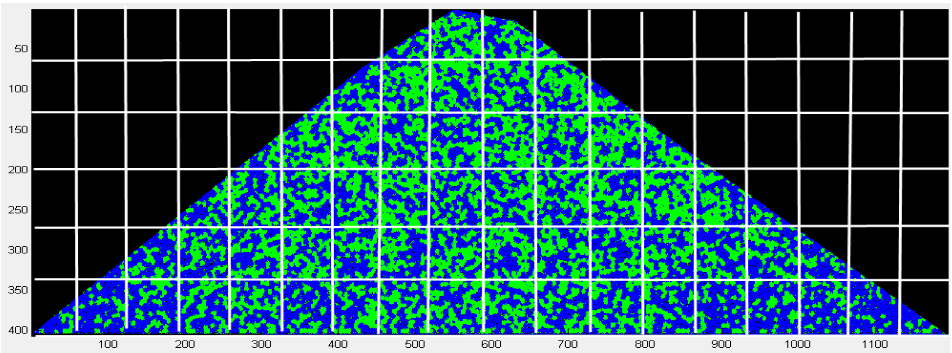

Fig. 8. A heap image, processed in MATLAB and divided into square bins, ready for image analysis. After indexing, BP and TAED particles are shown by blue and green colours, respectively.

The pixel number fraction for each constituent per bin, $\boldsymbol{C_{i_k}}$, is given by Equation 1:

$$\boldsymbol{C_{i_k}} = \frac{\boldsymbol{N_{i_k}}}{\sum_{i=1}^{m} \boldsymbol{N_{i_k}}} \quad \textbf{(1)}$$

where $\boldsymbol{N_{i_k}}$ is the number of pixels of the constituent i in the bin number k, with m being the total number of bins. The mean value, standard deviation, and coefficient of variation are given by Equations 2-4.

$$\mu_i = \frac{1}{n}\sum_{k=1}^{n} C_{i_k} \tag{2}$$

$$\sigma_i = \sqrt{\frac{1}{n}\sum_{k=1}^{n}\left(C_{i_k} - \mu_i\right)^2} \tag{3}$$

$$CoV_i = \frac{\sigma_i}{\mu_i} \tag{4}$$

2.5.2 Quantifying segregation based on particles number

Another method for quantifying the segregation, which is only applicable to simulation, is to count the particles number in each bin of the mixture. In this method the heap is discretised three-dimensionally into a number of bins (Fig. 9) in which the particle number fractions for species are calculated and their CoV for the entire heap is then obtained. A major advantage of this method is the ability to observe the segregation across the depth of the heap, i.e. the whole heap can be analysed three-dimensionally by DEM; while by image analysis only the segregation on the front face of the heap can be calculated.

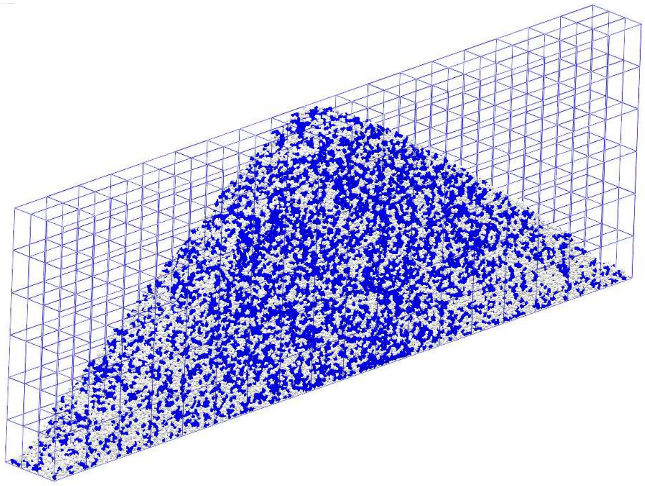

Fig. 9. The discretisation of the heap into bins in three dimensions to be used for measuring the coefficient of variation.

Calculating the CoV of the mixture components in randomly mixed system provides a suitable reference for comparison. To do so a random generator number is used in the Excel software to obtain random particle number fractions for each bin with regards to the mean value of 0.5 and the lower limit of standard deviation (randomly mixed) using Equation 5 [52, 56].

$$\sigma_R = \sqrt{\frac{\mathrm{P}(1-\mathrm{P})}{N}} \quad \textbf{(5)}$$

P is the probability of species and N is the total number of particles in the bin. The standard deviation of each bin is calculated separately as the number of the particles in the bins (e.g. corners and edges) are different, which affects the variability of the randomised mixture. After the random particle number fractions are generated for all the bins, the CoV of these fractions is calculated 100 times (with new random fractions) and the average is obtained.

3 Results

3.1 Simulation of segregation using clumped sphere approach

The process of heap formation of a binary mixture of BP and TAED is simulated using clumped sphere approach as shown earlier. A visual comparison between the results from the front view of the heap in experiment and the front and mid-plane views in DEM modelling is given in Fig. 10. Although the particle sizes of both species are in the same range, BP particles still show segregation near the corners of the heap at the front wall which might be due to the difference in shape or surface properties of the particles.

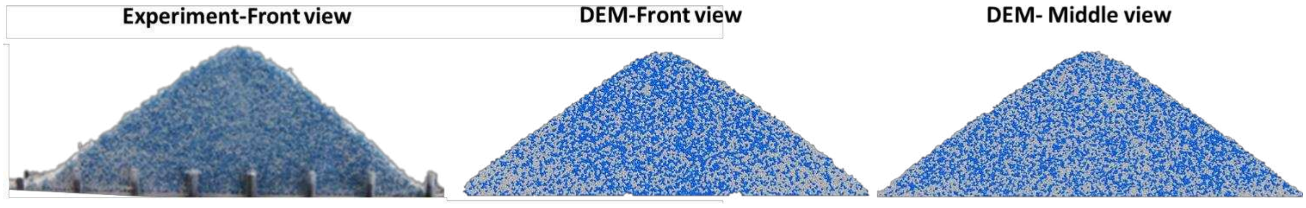

Fig. 10. Heap formation of binary mixture of the BP (beige/weight colour) and TAED (blue colour), for experiment and DEM modelling. (The photo of the experimental case shows a number of pins holding the front wall and are not within the bed.)

For analysing the experimental data, only the image analysis technique is used, while for the simulation results, both methods of image analysis (CLUMPED-Front view) and counting particle number (CLUMPED-Front layer), as described previously, are employed. For the latter, thin layers, having 2 mm width (2 times wider than the particles), from the front side and middle of the heap are selected, as shown in Fig. 11, and the particles are counted in each bin in these domains. Then the particles number fraction of the species at each bin ($\boldsymbol{C_{i_k}}$) for the front and middle layers of the heap are calculated and the values are depicted in format of contours to show the map of particles concentrations (Fig. 12).

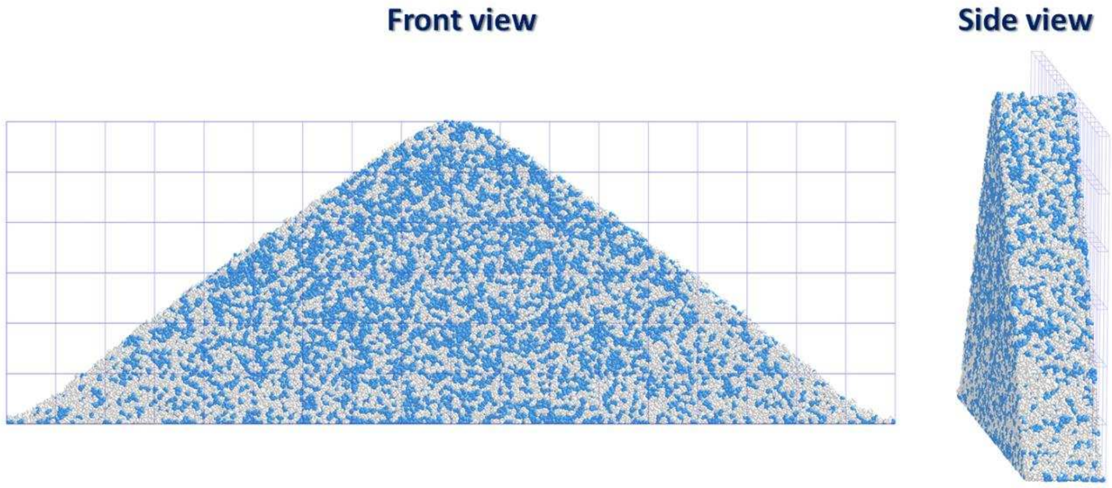

Fig. 11. A thin layer from the front side of the heap is selected and discretised.

As depicted in Fig. 12, the BP particles distribution at the front layer of the heap is clearly different from that of the middle layer. For the front layer, segregation of the BP particles is clearly visible in the corners of the heap, whereas for the middle layer, the particles are well mixed throughout the whole heap. The concentration map of the TAED particles has also the same visual pattern as of the BP; the only difference is that for the front layer, the corners have lower concentration values as the summation of $\boldsymbol{C}_{\boldsymbol{i}_{\boldsymbol{k}}}$ in each bin must be one. The central region, however, does not have much concentration difference (not shown).

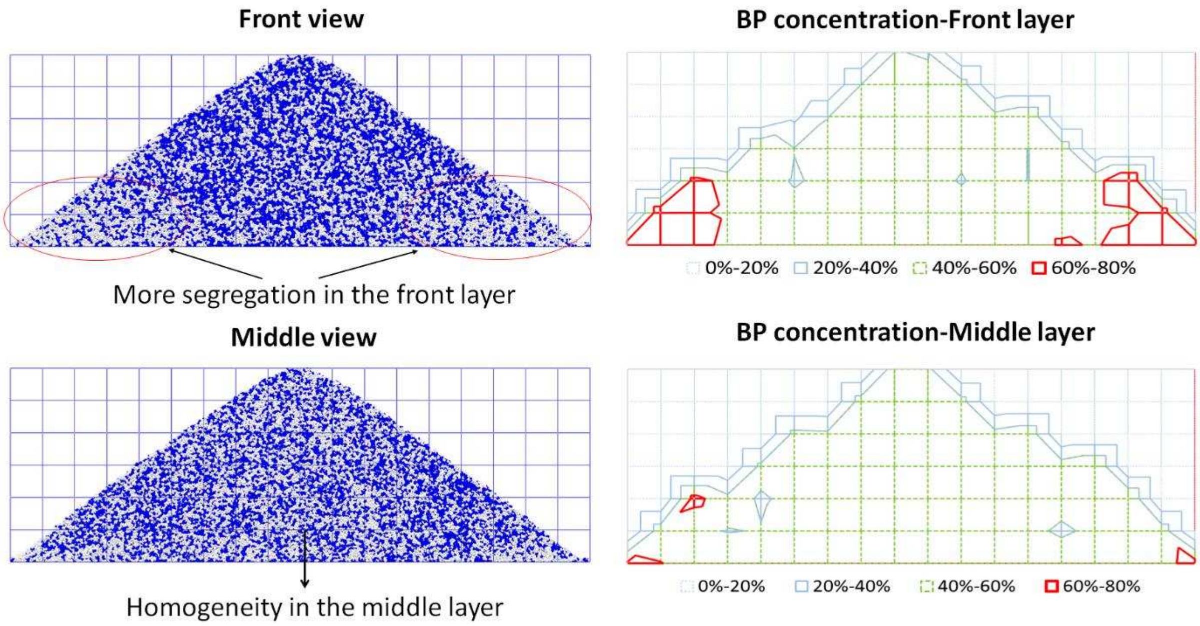

Fig. 12. Particles number concentration map of the PB particles for the front and middle layers of the heap (DEM simulation-clumped spheres approach).

The CoV of BP and TAED particles from these two analysis methods are presented in

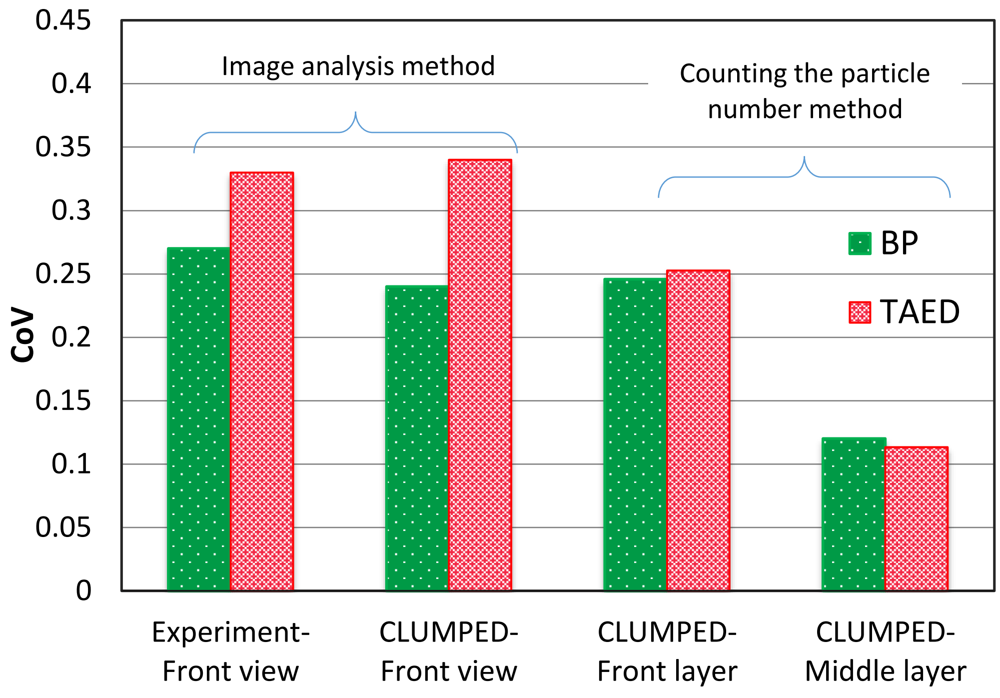

Fig. 13. A reasonable agreement between the experimental and numerical results is observable for both BP and TAED particles. The CoV of the BP particles is less than that of the TAED for both the experimental case and when the front view is analysed (i.e. CLUMPED-Front view). In contrast, the CoV obtained from the method of counting the particle number (i.e. CLUMPED-Front layer) is close for both species. The slight difference between the CoVs of the BP and TAED particles, observed in the image analysis method, is likely due to considering the projected area of the particles rather than the particles number. When 2D imaging is used to analyse the segregation, particles presentation on the screen is dependent on their packing style on the wall influenced by the particles aspect ratio, asperity, and surface roughness. This will lead to differences in the mean values of the colour pixels concentration on the wall and finally the value of the CoV for each species will be different. It is also likely that the use of a thin layer in the segregation analysis dilutes what is shown for the segregation tendency on the front

surface. This fact is observed in both experiment and DEM simulation, which shows that the simulation has been able to capture this effect.

It is also observed that the CoV of the middle layer of the heap is much lower than the CoV of the front layer (nearly half). As observed in Fig. 12 as well, particles have a very well-distribution in the middle of the heap in contrast to the front. In so far as the segregation in the heap front is concerned simulation with clumped sphere can reliably predict the extent of segregation.

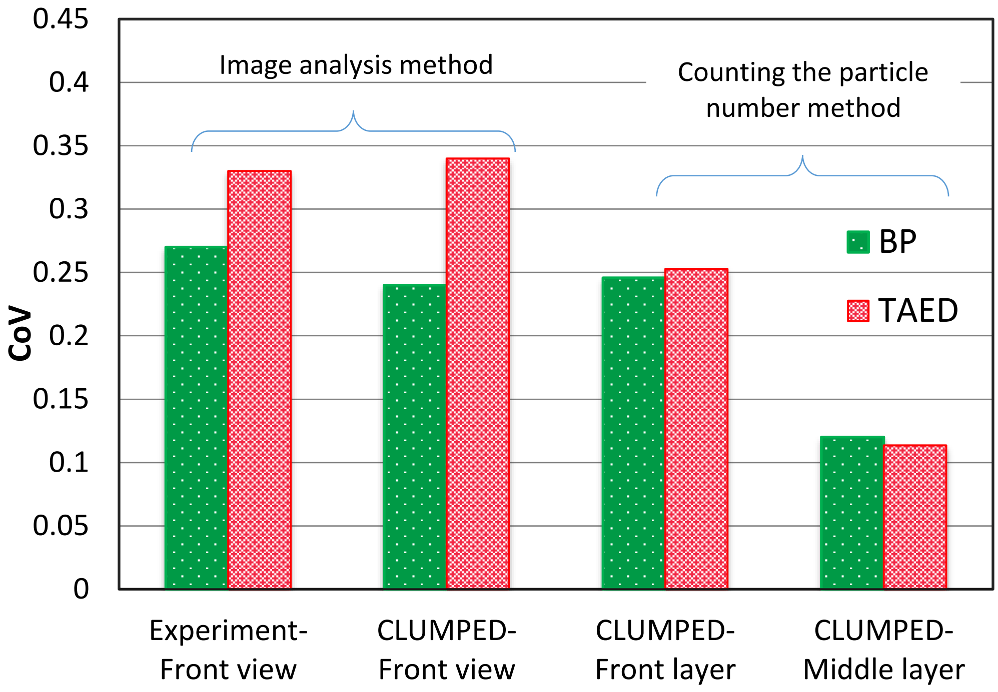

Fig. 13. CoV of BP and TAED particles obtained from experiments and clumped sphere approach using image analysis of the front view of the heap (CLUMPED-Front view) and counting particle number for the front layer (CLUMPED-Front layer) and the middle layer (CLUMPED-Middle layer).

3.2 Simulation of segregation using rolling friction approach

The rolling friction approach is used here to simulate the process of heap formation. Similar to the case of clumped-spheres the CoV of the particles obtained from the simulations using the rolling friction approach is analysed by image analysis and particle number methods. The results are shown in Fig. 14 and compared with the experimental data. Clearly the rolling friction approach underestimates the segregation tendency. ROLLING-Front view and ROLLING-Front layer results show the front of the heap analysed by the image analysis and counting particle number methods, respectively. ROLLING-Middle layer results show the condition in the middle of the heap based on counting the number of particles.

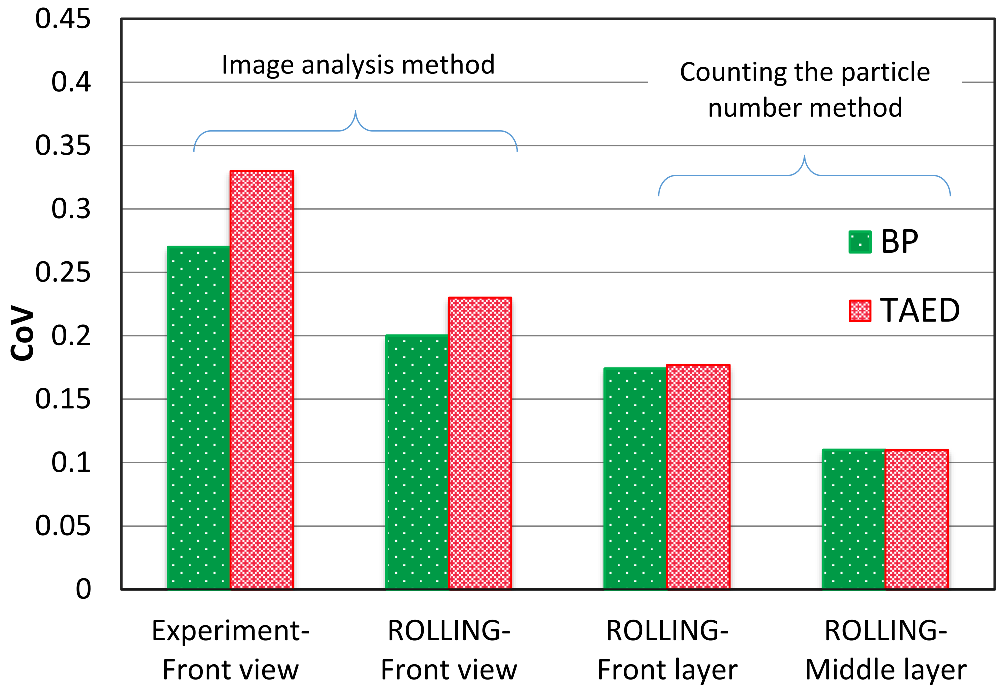

Fig. 14. CoV of BP and TAED particles obtained from experiments and rolling friction approach using image analysis at the front view of the heap (ROLLING-Front view), counting particle number for the front layer (ROLLING-Front layer) and the middle layer (ROLLING-Middle layer).

The segregation index for the mid-layer of the heap is much lower than that of the front layer. This is also clear from the particle number concentration map of the heap, shown in Fig. 15, where an extent of variation in concentration of BP particles is observable in the front layer of the heap. In contrast, the particles distribution in the middle of the heap is quite uniform. This difference between the particles distribution in the middle and front layers of the heap is likely due to the effect of particles shape at the wall. In fact wall and free surfaces facilitate the segregation by reducing the level of constraints imposed on the particles and hence the particles easily can rotate and segregate. This is not the case when the particles are subject to an interconnected mesh of particles restricting their movement, similar to what happens in the middle of the heap.

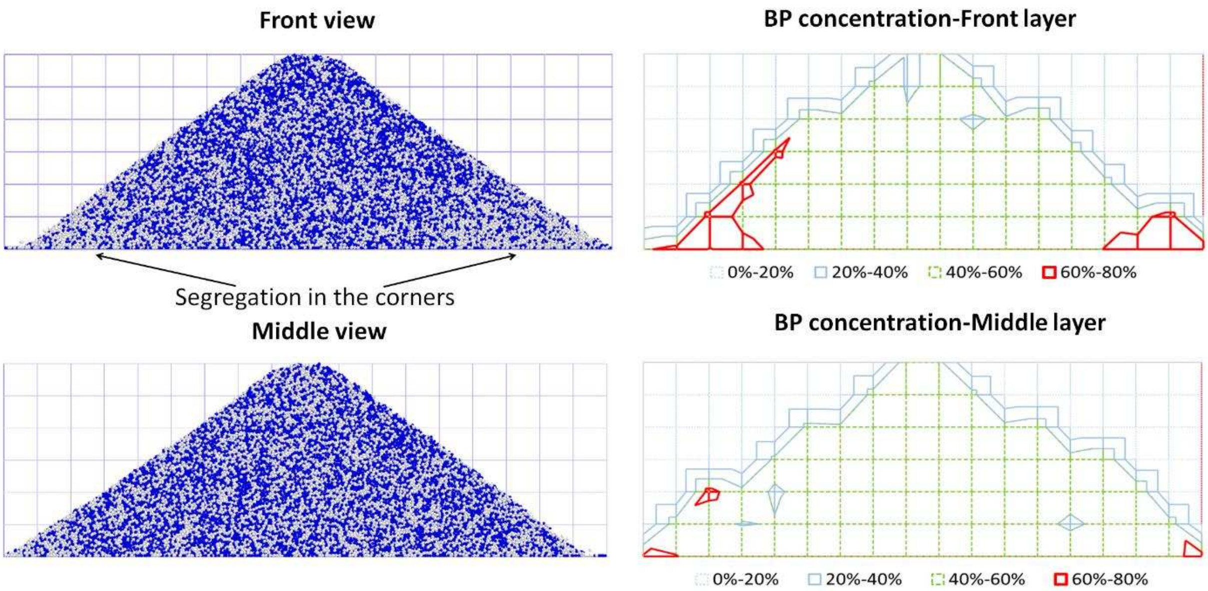

Fig. 15. BP particles (white) number concentration map for the front and middle layers of the heap (rolling friction approach).

Comparing Fig. 15 with the results obtained from the clumped sphere approach (Fig. 12), rolling friction approach gives slightly lower particle concentration in the corners of the heap.

The average values of the CoV for a randomly mixed system is calculated to be 0.14, 0.15, and 0.19 for the CLUMPED-front layer, ROLLING-front layer, and CLUMPED-front view cases. These numbers are between the CoV values of the front and middle layers showing that the middle layer is well mixed while the front layer has segregation. Also, the CoV values obtained by the rolling friction approach are some 35% lower than those of the experiments. The fact that the clumped sphere approach is predictive, while the rolling friction approach is not, most likely stems from the effect of particle-particle mechanical interlocking as well as the particles different aspect ratios and moment of inertia, which only happens in the real system and the clumped sphere approach. This can be observed clearly from a close-up images of the particles at the front view of the heap as shown in Fig. 16. Different shapes give different behaviours during the packing and an extra effect of the bed dilation during the particles rotation [57]. The difference observed between the arrangements of particles in these two approaches shows that the effect of particle shape is not limited to the rolling mechanism of the particles, rather it affects the particles contacts in a more complex network.

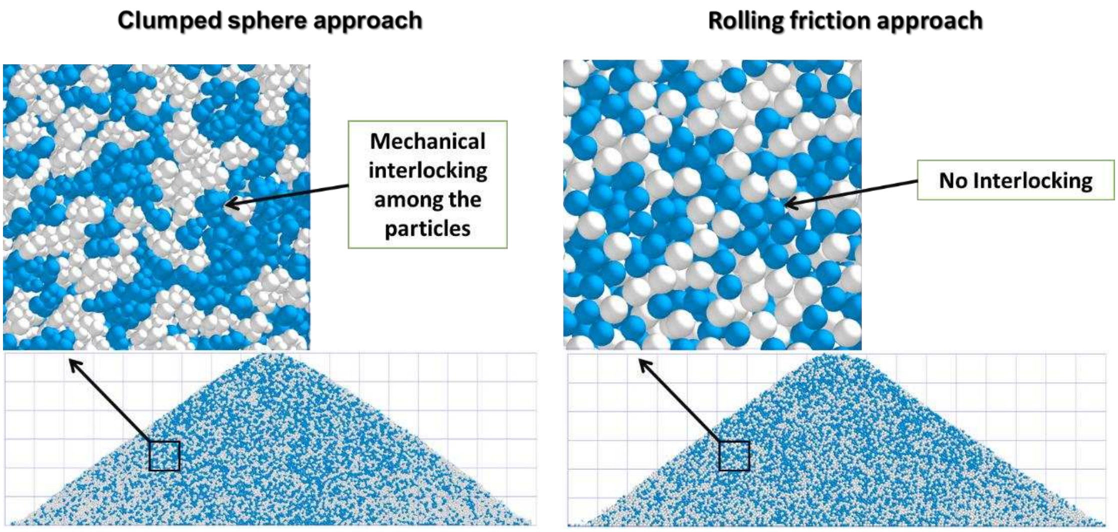

Fig. 16. Arrangements of the BP (white) and TAED (blue) particles at the heap front, simulated by the clumped sphere and rolling friction approaches.

4 Conclusions

The segregation of a binary powder mixture during the heap formation is modelled numerically using the DEM method. Two main ingredients of washing powders, namely BP and TAED are used as model test materials. Clumped spheres and rolling friction approaches are utilised for modelling the particles segregation and the results are compared with the experiment. It is observed that particles repose angle is highly dependent on the particle shape and there is a minimum number of spheres which gives adequate comparison, after which not much improvement is obtained. The results obtained from DEM simulations show that the clumped sphere approach is a predictive tool for simulating the segregation during the heap formation. In contrast, the rolling friction approach underestimates the segregation tendency even when it is tuned to predict the repose angle. It is also observed that the middle and front layers of the heap give two different predictions of the segregation tendency. Thus the particles distribution pattern at the front view of the heap is not well representative of the condition of the whole mixture.

Calibrated rolling friction as a substitute for particle shape is not an accurate approximation of irregular particles for the simulation of segregation behaviour, even for a system which is not much prone to segregation. This situation becomes exacerbated when segregation due to size difference becomes more extensive, as will be reported in future works.

5 Acknowledgments:

This work is part of Chariot, funded by the UK government’s Advanced Manufacturing Supply Chain Initiative (AMSCI) [grant number 31587, 233189]. The authors are also grateful to Drs Massih Pasha and Umair Zafar and Mrs Claire Duckitt for their help and guidance.

6 References

[1] A.-N. Huang, H.-P. Kuo, Developments in the tools for the investigation of mixing in particulate systems – A review, Adv Powder Technol, 25 (2014) 163-173.
[2] J. Ottino, D. Khakhar, Mixing and segregation of granular materials, Annu Rev Fluid Mech, 32 (2000) 55-91.
[3] A. Shimoska, I. Nousou, Y. Shirakawa, J. Hidaka, Effect of Particle Shape on Size Segregation of Particles, Chem Engineer Trans, 32 (2013) 2143-2148.
[4] A. Shimosaka, Y. Shirakawa, J. Hidaka, Effects of Particle Shape and Size Distribution on Size Segregation of Particles, J Chem Eng Jpn, 46 (2013) 187-195.
[5] J.M. Ottino, D.V. Khakhar, Mixing and segregation of granular materials, Annu Rev Fluid Mech, 32 (2000) 55-91.
[6] A. Dziugys, R. Navakas, The role of friction in mixing and segregation of granular material, Granul Matter, 11 (2009) 403-416.
[7] A. Hassanpour, M. Eggert, M. Ghadiri, Analysis of segregation of binary mixtures of particulate solids due to size, density and cohesion, The 6th International Conference on Micro-mechanics of Granular Media, Powders and Grains 2009Golden Colorado, USA, 2009, pp. 687-690.
[8] K.A. Gillemot, E. Somfai, T. Borzsonyi, Shear-driven segregation of dry granular materials with different friction coefficients, Soft Matter, 13 (2017) 415-420.
[9] S. Yu, Y. Guo, C.Y. Wu, DEM/CFD modelling of the deposition of dilute granular systems in a vertical container, Chinese Sci Bull, 54 (2009) 4318-4326.
[10] S.K. Hajra, D. Shi, J.J. McCarthy, Granular mixing and segregation in zigzag chute flow, Phys Rev E, 86 (2012) 061318.
[11] D. Brone, F.J. Muzzio, Size segregation in vibrated granular systems: A reversible process, Phys Rev E, 56 (1997) 1059-1063.
[12] C.M. Dury, R. Knecht, G.H. Ristow, Size segregation of granular materials in a 3D rotating drum, High-Performance Computing and Networking, 1401 (1998) 860-862.
[13] A. Dziugys, R. Navakas, The role of friction on size segregation of granular material, Mechanika, (2007) 59-68.
[14] L.B.H. May, L.A. Golick, K.C. Phillips, M. Shearer, K.E. Daniels, Shear-driven size segregation of granular materials: Modeling and experiment, Phys Rev E, 81 (2010).
[15] Y. Guo, C.Y. Wu, C. Thornton, The effects of air and particle density difference on segregation of powder mixtures during die filling, Chem Eng Sci, 66 (2011) 661-673.
[16] E.W.C. Lim, Density Segregation of Binary Granular Mixtures in Bumpy Vibrated Beds, Cbee 2009: Proceedings of the 2009 International Conference on Chemical, Biological and Environmental Engineering, (2010) 8-12.
[17] E.W.C. Lim, Density Segregation in Vibrated Granular Beds with Bumpy Surfaces, Aiche J, 56 (2010) 2588-2597.
[18] Y. Fan, K.V. Jacob, B. Freireich, R.M. Lueptow, Segregation of granular materials in bounded heap flow: A review, Powder Technol, 312 (2017) 67-88.
[19] S.J. Roskilly, E.A. Colbourn, O. Alli, D. Williams, K.A. Paul, E.H. Welfare, P.A. Trusty, Investigating the effect of shape on particle segregation using a Monte Carlo simulation, Powder Technol, 203 (2010) 211-222.

[20] P. Tang, V.M. Puri, Segregation quantification of two-component particulate mixtures: Effect of particle size, density, shape, and surface texture, Particul Sci Technol, 25 (2007) 571-588.
[21] R. Moreno-Atanasio, R.A. Williams, X. Jia, Combining X-ray microtomography with computer simulation for analysis of granular and porous materials, Particuology, 8 (2010) 81-99.
[22] R. Escudié, N. Epstein, J.R. Grace, H.T. Bi, Effect of particle shape on liquid-fluidized beds of binary (and ternary) solids mixtures: segregation vs. mixing, Chemical Engineering Science, 61 (2006) 1528-1539.
[23] Y. Fan, C.P. Schlick, P.B. Umbanhowar, J.M. Ottino, R.M. Lueptow, Modelling size segregation of granular materials: the roles of segregation, advection and diffusion, J Fluid Mech, 741 (2014) 252-279.
[24] J.M.N.T. Gray, C. Ancey, Multi-component particle-size segregation in shallow granular avalanches, J Fluid Mech, 678 (2011) 535-588.
[25] M.B. Hu, Q.S. Wu, R. Jiang, Size segregation in a vibrated tilted compartmentalized granular chamber, Chinese Phys Lett, 20 (2003) 1091-1093.
[26] D. Mateo-Ortiz, F.J. Muzzio, R. Mendez, Particle size segregation promoted by powder flow in confined space: The die filling process case, Powder Technol, 262 (2014) 215-222.
[27] A. Rosato, K.J. Strandburg, F. Prinz, R.H. Swendsen, Why the Brazil nuts are on top: Size segregation of particulate matter by shaking, Phys Rev Lett, 58 (1987) 1038-1040.
[28] A. Thornton, T. Weinhart, S. Luding, O. Bokhove, Modeling of Particle Size Segregation: Calibration Using the Discrete Particle Method, Int J Mod Phys C, 23 (2012).
[29] S.L. Wu, M.Y. Kou, J. Xu, X.Y. Guo, K.P. Du, W. Shen, J. Sun, DEM simulation of particle size segregation behavior during charging into and discharging from a Paul-Wurth type hopper, Chem Eng Sci, 99 (2013) 314-323.
[30] G. Lu, J.R. Third, C.R. Müller, Discrete element models for non-spherical particle systems: From theoretical developments to applications, Chem Eng Sci, 127 (2015) 425-465.
[31] C.M. Wensrich, A. Katterfeld, Rolling friction as a technique for modelling particle shape in DEM, Powder Technol, 217 (2012) 409-417.
[32] C. Goniva, C. Kloss, N.G. Deen, J.A.M. Kuipers, S. Pirker, Influence of rolling friction on single spout fluidized bed simulation, Particuology, 10 (2012) 582-591.
[33] M.A. Behjani, N. Rahmanian, N. Fardina bt Abdul Ghani, A. Hassanpour, An investigation on process of seeded granulation in a continuous drum granulator using DEM, Adv Powder Technol.
[34] M. Combarros, H.J. Feise, H. Zetzener, A. Kwade, Segregation of particulate solids: Experiments and DEM simulations, Particuology, 12 (2014) 25-32.
[35] J.F. Favier, M.H. Abbaspour-Fard, M. Kremmer, A.O. Raji, Shape representation of axi-symmetrical, non-spherical particles in discrete element simulation using multi-element model particles, Engineering Computations (Swansea, Wales), 16 (1999) 467-480.
[36] M. Pasha, C. Hare, M. Ghadiri, A. Gunadi, P.M. Piccione, Effect of particle shape on flow in discrete element method simulation of a rotary batch seed coater, Powder Technol, 296 (2016) 29-36.
[37] W.H. Hager, Wilfrid Noel Bond and the Bond number, J Hydraul Res, 50 (2012) 3-9.
[38] K.L. Johnson, K. Kendall, A.D. Roberts, Surface Energy and the Contact of Elastic Solids, Proceedings of the Royal Society of London A: Mathematical, Physical and Engineering Sciences, 324 (1971) 301-313.
[39] H. Hertz, Ueber die Berührung fester elastischer Körper (on the contact of elastic solids), Journal für die reine und angewandte Mathematik (Crelle's Journal), 1882, pp. 156–171.

[40] H. Deresiewicz, R.D. Mindlin, U. Columbia, E. Department of Civil, Elastic spheres in contact under varying oblique forces, 1952.
[41] A. Di Renzo, F.P. Di Maio, Comparison of contact-force models for the simulation of collisions in DEM-based granular flow codes, Chemical Engineering Science, 59 (2004) 525-541.
[42] M.M. Martín, Introduction to software for chemical engineers, CRC Press2014.
[43] C. Thornton, Granular Dynamics, Contact Mechanics and Particle System Simulations, Springer2015.
[44] M. Price, V. Murariu, G. Morrison, Sphere clump generation and trajectory comparison for real particles, Proceedings of Discrete Element Modelling 2007, (2007).
[45] J. Ai, J.-F. Chen, J.M. Rotter, J.Y. Ooi, Assessment of rolling resistance models in discrete element simulations, Powder Technol, 206 (2011) 269-282.
[46] L.T. Fan, R.H. Wang, On mixing indices, Powder Technol, 11 (1975) 27-32.
[47] D.K. Rollins, D.L. Faust, D.L. Jabas, A superior approach to indices in determining mixture segregation, Powder Technol, 84 (1995) 277-282.
[48] R. Hogg, Characterization of relative homogeneity in particulate mixtures, Int J Miner Process, 72 (2003) 477-487.
[49] S.-H. Chou, Y.-L. Song, S.-S. Hsiau, A Study of the Mixing Index in Solid Particles, Kona Powder Part J, (2016) 2017018.
[50] B.N. Asmar, P.A. Langston, A.J. Matchett, A generalised mixing index in distinct element method simulation of vibrated particulate beds, Granul Matter, 4 (2002) 129-138.
[51] G.R. Chandratilleke, A.B. Yu, J. Bridgwater, K. Shinohara, A particle-scale index in the quantification of mixing of particles, Aiche J, 58 (2012) 1099-1118.
[52] P.M.C. Lacey, The mixing of solid particles, Chemical Engineering Research and Design, 75 (1997) S49-S55.
[53] A. Kukukova, J. Aubin, S.M. Kresta, A new definition of mixing and segregation: Three dimensions of a key process variable, Chemical Engineering Research and Design, 87 (2009) 633-647.
[54] A. Kukuková, B. Noël, S.M. Kresta, J. Aubin, Impact of sampling method and scale on the measurement of mixing and the coefficient of variance, Aiche J, 54 (2008) 3068-3083.
[55] M. Pasha, Segregation image analysis by MATLAB code Personal communication, 2016.
[56] M.J. Rhodes, Introduction to particle technology, John Wiley & Sons2008.
[57] L.B. May, L.A. Golick, K.C. Phillips, M. Shearer, K.E. Daniels, Shear-driven size segregation of granular materials: Modeling and experiment, Phys Rev E, 81 (2010) 051301.

Table captions

Table 1: Physical properties of BP and TAED particles used in DEM simulations.

Table 2: Specifications of the modelling and particle shape.

Table 3: Calibrated coefficient of rolling friction for the spherical particles.

Figure captions

Fig. 1. Geometry utilised in DEM simulations based on the geometry of the experimental set up.

Fig. 2. Typical shapes of (a) BP (white) and (b) TAED (blue) particles sieved between 850 and 1000 **μ**m.

Fig. 3. Schematic diagram for measuring the coefficient of sliding friction. Graph (a) shows the surfaces at rest, graph (b) shows the particle-particle sliding friction experiment, and graph (c) depicts the particle-wall sliding experiment.

Fig. 4. The non-spherical TAED particle shape representation by increasing the number of spheres (TAED particles' size range: 850-1000 μm).

Fig. 5. DEM simulation of a TAED particle heap using 5-sphere clump model. (Particle size range: 850-1000 μm).

Fig. 6. The effect of number of spheres in the clumped-spheres model on the heap repose angle

Fig. 7. The procedure of calibrating the spheres rolling friction against the angle of repose.

Fig. 8. A heap image, processed in MATLAB and divided into square bins, ready for image analysis. After indexing, BP and TAED particles are shown by blue and green colours, respectively.

Fig. 9. The discretisation of the heap into bins in three dimensions to be used for measuring the coefficient of variation.

Fig. 10. Heap formation of binary mixture of the BP (beige/weight colour) and TAED (blue colour), for experiment and DEM modelling. (The photo of the experimental case shows a number of pins holding the front wall and are not within the bed.)

Fig. 11. A thin layer from the front side of the heap is selected and discretised.

Fig. 12. Particles number concentration map of the PB particles for the front and middle layers of the heap (DEM simulation-clumped spheres approach).

Fig. 13. CoV of BP and TAED particles obtained from experiments and clumped sphere approach using image analysis at the front view of the heap (CLUMPED-Front view), counting particle number for the front layer (CLUMPED-Front layer) and the middle layer (CLUMPED-Middle layer).

Fig. 14. CoV of BP and TAED particles obtained from experiments and rolling friction approach using image analysis at the front view of the heap (ROLLING-Front view), counting particle number for the front layer (ROLLING-Front layer) and the middle layer (ROLLING-Middle layer).

Fig. 15. BP particles (white) number concentration map for the front and middle layers of the heap (rolling friction approach).

Fig. 16. Arrangements of the BP (white) and TAED (blue) particles at the heap front, simulated by the clumped sphere and rolling friction approaches.